



Transient liquid phase bonding of stainless steel 316 L to Ti-6Al-4 V using Cu/Ni multi-interlayer: microstructure, mechanical properties, and fractography

A. Surendar¹ · Andrew Lucas² · Mazhar Abbas³ · Robbi Rahim⁴ · Mohammad Salmani⁵

Received: 24 October 2018 / Accepted: 5 April 2019 / Published online: 28 April 2019
© International Institute of Welding 2019

Abstract

In the present work, transient liquid phase bonding (TLP) of stainless steel 316 L to Ti-6Al-4 V using simultaneously both Cu and Ni interlayers was performed and effect of bonding temperature (950 to 1050 °C) on microstructure and mechanical properties of the joints was studied. The joint zones were analyzed using scanning electron microscopy (SEM) equipped with energy dispersive spectroscopy (EDS). Microhardness and shear strength tests were also applied to evaluate the mechanical properties of the joints. The results showed that various eutectic phases and intermetallic compounds were formed at the interface; however, diversity of intermetallics was different in the joint zone for each specimen which can be due to the bonding temperature and type of eutectic phase transformation. The more increase of bonding temperature to higher than 1000 °C, the more deterioration in mechanical properties of the bonded joints is led so that the shear strength decreased from 385 MPa (maximum value) to 257 MPa.

Keywords Diffusion · Eutectic · Hardness · Shear strength · Solidification

1 Introduction

The ever-increasing demand for fabrication of hybrid structures with the good mechanical properties and superior corrosion resistance leads to a widespread interest among researchers to develop joining technology of binary systems [1–3]. It is found that the great differences in structural heterogeneity as well as mismatch in the physical properties are great challenges to produce Ti/steel joints by conventional

welding processes [4, 5]. To overcome this problem, advance fusion welding techniques have been proposed [6–9]. However, formation of the excessive intermetallic compounds and microcracks deteriorates the microstructure and the mechanical behaviors of the joints. The diffusion bonding process, as an alternative method, has been recently developed to join steel/Ti couples [10–12]. The extensive studies have shown that the presence of an interlayer makes a significant improvement in the mechanical properties of Ti/steel joints which is due to the decrease in formation rate of brittle intermetallic compounds at the interface. Hence, interlayers with the various chemical compositions have been applied to amend the joint features. For instance, Yildiz et al. [13] investigated the diffusion bonding of pure Ti and ferritic steel using Ni interlayer and found that the Ni/steel interface is the vulnerable part of joint zone. Balasubramanian [14–16] extensively studied the diffusion bonding of steel/Ti joint using Ag interlayer. It is reported that the temperature bonding range of 750–800 °C leads to the highest joint quality with shear strength of 149 MPa. Shrinkage-stress assisted diffusion bonding, as a novel technique, was proposed by Mukherjee et al. [17] to join titanium and stainless steel which facilitates the diffusion bonding at the interfaces inside the grooves. Wang et al. [18] also introduced an impulse pressuring

Recommended for publication by Commission III - Resistance Welding, Solid State Welding, and Allied Joining Process

✉ Mohammad Salmani
salmanimohammad253@gmail.com

¹ Department of Electronics and Communication Engineering, Vignan's Foundation for Science Technology and Research, Guntur, India

² Indian Institute of Technology Bombay, Mumbai, India

³ Department of Management Sciences, COMSATS University Islamabad Vehari Campus, Vehari, Punjab, Pakistan

⁴ Sekolah Tinggi Ilmu Manajemen Sukma, Medan, Indonesia

⁵ Payameh Noor University, Tehran branch, Tehran, Iran

diffusion bonding technology to fabricate a steel/Ti couple using Ni interlayer. It is found that the interdiffusion between base materials can be efficiently restricted via this technique. In general, an interlayer delays the interdiffusion of Ti and Fe into the base metals and controls formation of brittle Fe–Ti compounds in the joint zone. The liquid state diffusion bonding has been also taken a wide interest to join Ti/steel systems, because the bonding process can be carried out with low bonding pressure and short holding time [19, 20]. This technique facilitates the interdiffusion of elements along the interface due to the presence of a liquid phase in the joint zone. The application of multi-interlayer is another method to control the chemical heterogeneity at the interface. For example, using Cu/Nb multi-interlayer to weld Ti64 and SS316 makes a joint with high tensile strength of 489 MPa; however, with the increase of temperature above 900 °C, intermetallic formation intensifies at the interface [17]. Li et al. [12] applied Nb/Cu/Ni structure as multi-interlayer to bond Ti/SS couple. It was found that the Cu–Nb solution strengthening effect improves the mechanical properties of joint. Kundu et al. [21] carried out the solid state diffusion bonding of duplex SS to Ti64 by a composite Ni/Cu interlayer. The Cu layer, adjacent to Ti alloy, produced various types of Cu–Ti intermetallic compounds in the joint zone.

As aforementioned, a suitable selection of multi-interlayer can ameliorate the transitional physical properties between the parent metals and control the types of intermetallic compounds in the joint zone. In this work, we used a Cu/Ni multi-interlayer to join the stainless steel to Ti64 with transient liquid phase technique. The designing of the joined system in the form of Ti64/Ni/Cu/SS will lead to the formation of Ni–Ti eutectic liquid above the ~940 °C at the interface, while the neighboring of Cu and Fe will control the intermetallic phases at the Cu/SS interface. Moreover, the multi-interlayer can also impede the growth of intermetallic compounds with formation of multiple metallic phases at the interface.

2 Materials and methods

In order to join stainless steel 316 L (17.1 Cr–11.7 Ni–2.5 Mo–2.4Mn–1Si–0.04 C–bal. Fe) to Ti–6Al–4 V (6.1Al–4.1 V–bal. Ti), pure Cu and Ni foils were simultaneously employed as the interlayer, as shown in Fig. 1. The thickness of Cu is 100 µm, while Ni has a lower thickness (50 µm). The lower melting point of Cu provides more transient liquid phase at the interface. As a result, we used a thicker Cu layer to facilitate the TLP bonding process in the joint zone. Prior to bonding process, specimens were prepared with the dimension of 10 × 10 × 5 mm³ and faying surfaces to be joined were ground by SiC papers in several stages. An induction furnace with argon atmosphere (flow rate of 15 L/min) was used to avoid any

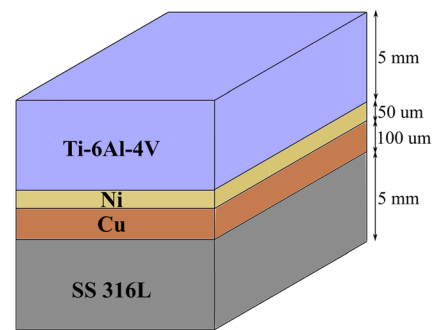


Fig. 1 Schematic of the joint

oxidation in the joint zone. The holding pressure and bonding time were fixed at 2 MPa and 30 min, respectively while the bonding temperature values were 950, 1000, and 1050 °C. After the joining process, optical microscope (OM) and scanning electron microscope were applied to characterize the microstructure of joint zone. The mechanical properties were evaluated by microhardness and shear strength tests. Hardness measurements of various areas across the joint were conducted by a Vickers tester with a load of 50 g. The shear strength of the joints was also measured according to ASTM standard D1002-99 at room temperature.

3 Results and discussion

3.1 Microstructure evaluation and phase transformation

Bonding temperature is one of the key factors in TLP bonding deeply affecting microstructure and mechanical properties of the joints. It is believed that unique phase transformations happen at the selected bonding temperatures so that different metallic phases can form at the interface. Figure 2 shows SEM micrograph of a bond made at 950 °C. It can be clearly seen that the joint zone is divided into three distinct regions. Higher degree of Ni diffusion into the Ti leads to formation of a Widmanstätten microstructure adjacent to the Ti alloy (region 1). In general, nickel and copper are inherently β -stabilizing elements so their diffusion into Ti–6Al–4 V decreases α - β eutectoid transformation and forms a needle-like microstructure at the Ti alloy interface [19, 20, 22]. Chemical composition of region 1 also confirms the possibility of eutectoid structure (see Table 1). Considering Fig. 2b, a distinguished microstructure is observed at the center of the joint zone. At 950 °C, a eutectic transformation provides liquid at the interface. This liquid is arising from a phenomenon, named dissolution, in TLP bonding. In this case, liquefaction will begin in the joint zone where, through interdiffusion of interlayer elements and Ti, a region is created at the eutectic composition. In fact, migration of Ni and Cu across the joint zone leads to

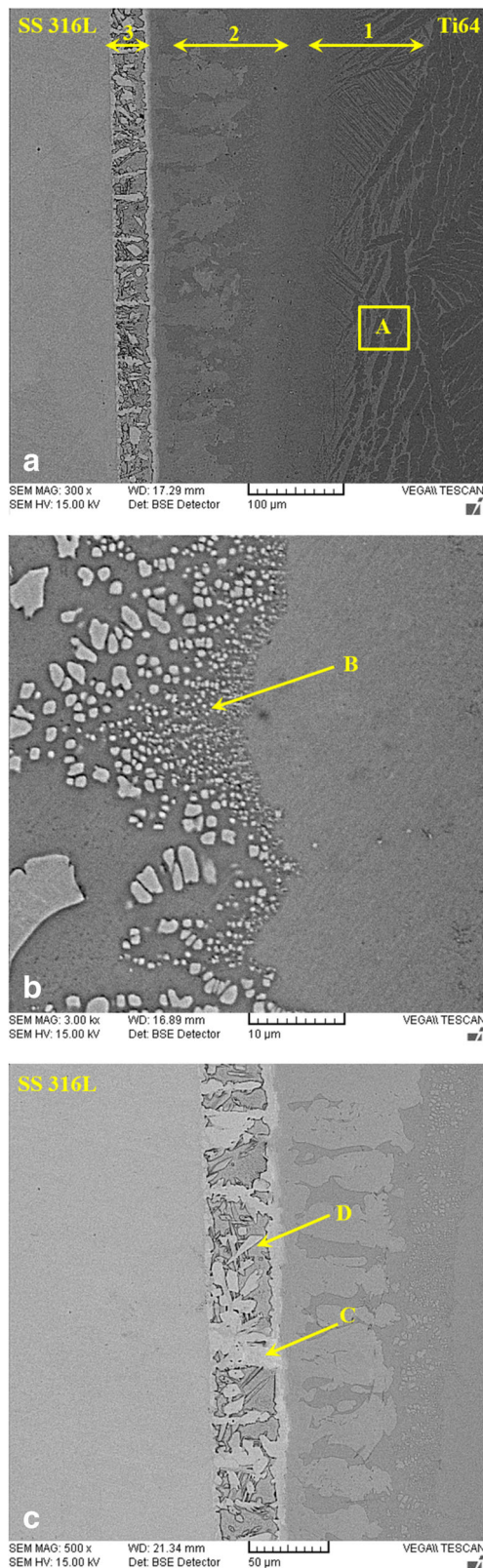


Fig. 2 SEM micrograph of the bond made at 950 °C. **a** Ti side. **b** Joint center. **c** Steel side

Table 1 EDS analysis (Wt.%) of selected regions in SEM micrographs

	Fe	Al	Cu	Ti	V	Ni	Cr	Mo	Mn
A	0.02	4.25	2.1	83.41	3.92	6.30	0	0	0
B	0.09	0.1	42.55	45.27	0.04	11.53	0.12	0.08	0.02
C	72.06	0.05	0.3	2.3	0	4.23	15.75	3.21	2.1
D	51.21	0	9.95	19.63	0	11.8	5.36	1.05	1
E	0.19	0.14	16.74	37.76	0.03	44.65	0.39	0.05	0.05
F	0	3.83	4.9	77.18	3.85	10.24	0	0	0
G	0.3	0.09	15.74	56.64	0.8	26.17	0.43	0.17	0.04

dissolution of Ti and growth of liquid at the interface. According to EDS analysis and ternary phase diagram of Cu–Ni–Ti [23], the eutectic phases formed in this region can be $\beta 1$ (NiTi), ϕ (CuTi), and Δ (CuNiTi).

Figure 2 c illustrates that microstructure at the steel interface is much different from the Ti side. The EDS analysis from this part shows that diffusion of Fe into the joint zone is restricted to a thin reaction layer with thickness of 50 μm along the stainless steel. Region C mainly consists of Fe alloys while a considerable amount of Cu, Ni, and Ti is found in region D. It reveals that formation of liquid in the joint zone makes easier migration of Ti towards the Fe alloy so that a Ti-rich region is formed at the stainless steel interface. It is suggested that presence of Ni in the joint zone leads to reduction in eutectic temperature and increase in formation of liquid at the interface. Hence, diffusion of Ti along the joint zone would be more perceptible in Fe/Cu/Ni/Ti system at 950 °C.

SEM micrograph of a bond made at 1000 °C is presented in Fig. 3. As clear in the figure, formation of Widmanstatten structure at the Ti alloy interface and a thin reaction layer along the stainless steel is similar to the bond made at 950 °C; however, microstructure in the joint center is completely different. The zonal EDS analysis of this region indicates that chemical distribution across the joint zone along with increase of bonding temperature make changes in the microstructure. According to the Cu–Ni–Ti ternary phase diagram [23] and chemical analyses (see Table 1), a eutectic transformation is occurred in the joint zone which is due to interdiffusion of Ti, Ni, and Cu across the interface. Formation of $\beta 1$ (NiTi), Δ (CuNiTi), and ι (Ni₃Ti) is outcome of the eutectic transformation in bonding temperature of 1000 °C. It should be noted that nickel plays a vital role in this eutectic transformation so that a substantial amount of Ni (42% wt.) is used to form eutectic phases while only 12% wt. Ni takes part in the eutectic transformation at 950 °C.

Figure 4 demonstrates SEM micrograph of a bond made at 1050 °C. As it is observed, the eutectoid region is coarser and more extensive than that of Figs. 2 and 3 which is owing to higher bonding temperature and exponential increase in diffusivity of Ni

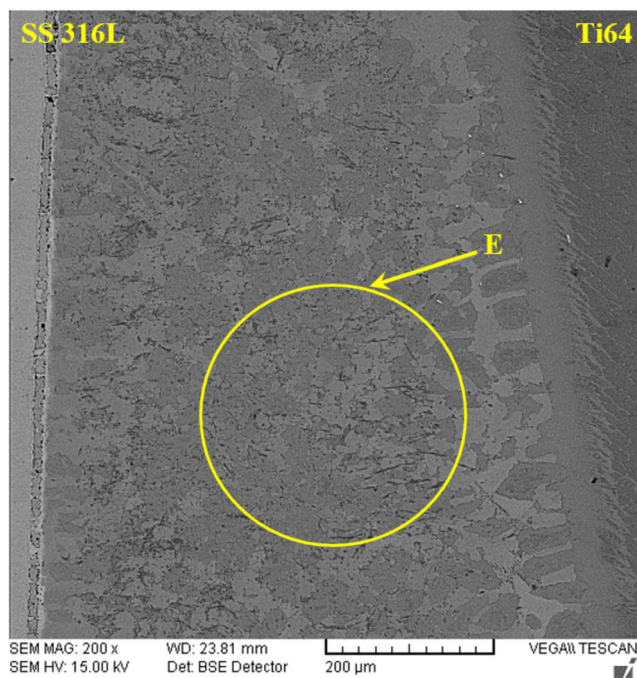


Fig. 3 SEM micrograph of a bond made at 1000 °C

and Cu into the Ti alloy. Considering the chemical composition of the joint center and Cu–Ni–Ti ternary phase diagram [23], the eutectic transformation with components of $\iota + \Delta + \gamma + L$ dominates in the joint zone. Hence, the eutectic-like structure in the joint may result by formation of ι (Ni_3Ti), Δ (CuNiTi), and γ (Ni, Cu) phases. A significant participation of nickel and copper in formation of eutectic structure in the center of the bond and eutectoid structure at the Ti interface can be the main reason for

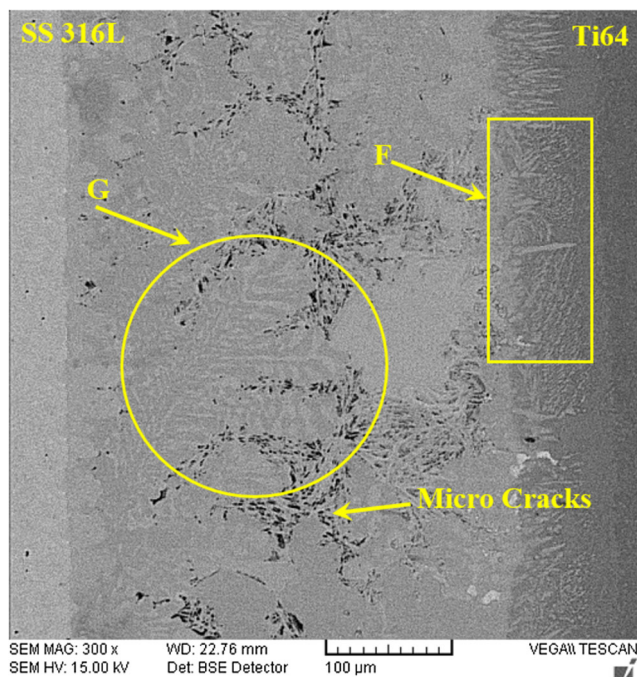


Fig. 4 SEM micrograph of a bond made at 1050 °C

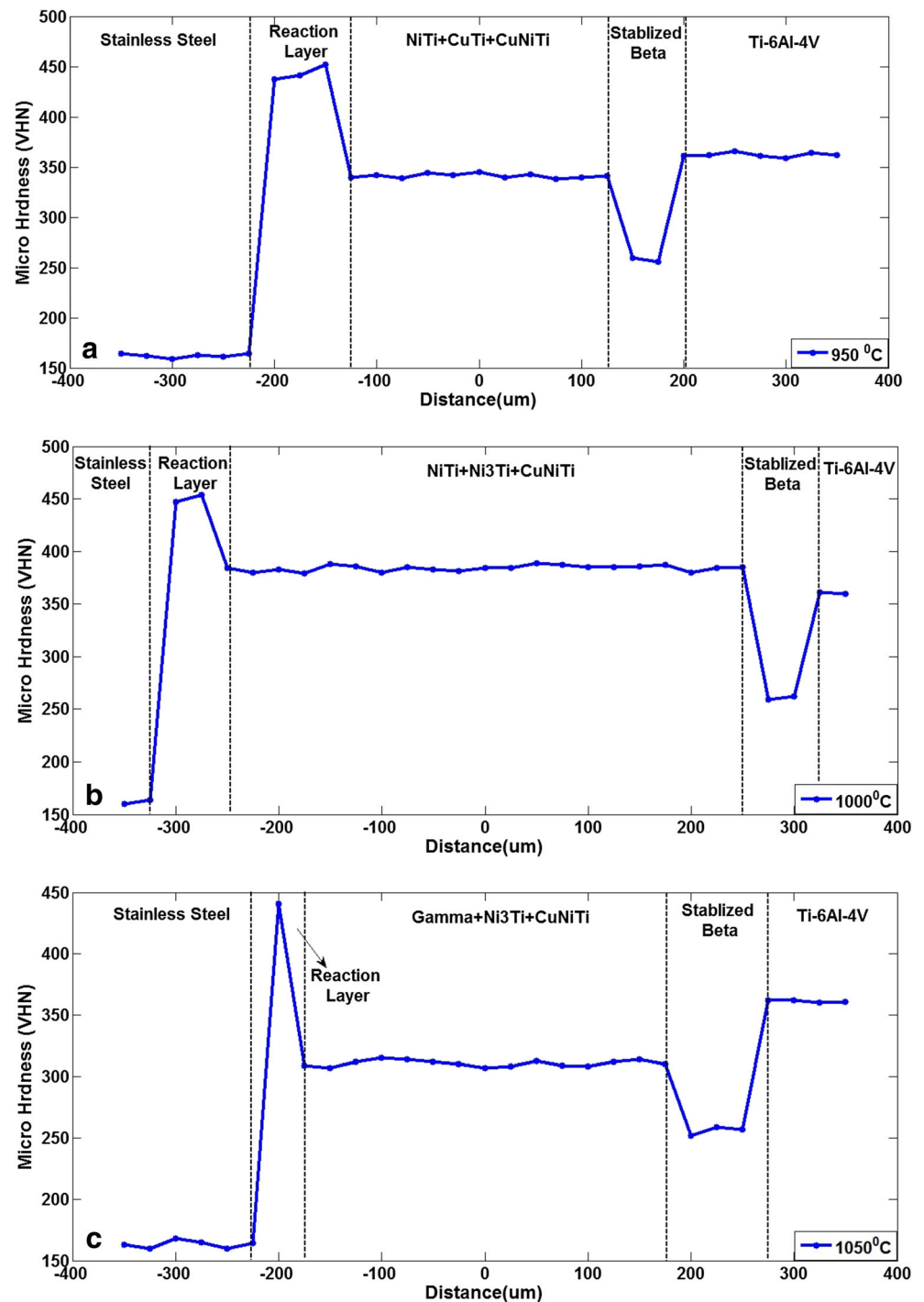
narrowing of the known reaction layer along the stainless steel. It is considered that the higher bonding temperature can create an opportunity for eutectic phases to grow more extensive across the joint zone. The existence of voids and microcracks in the joint zone of sample made at 1050 is another point that should be noticed. It is believed that growth of eutectic microstructure in high temperatures is led by shrinkage of melted phase at the interface during athermal solidification; hereupon, formation of microcracks and microvoids in the joint can be expected. This occurrence in the joint zone indicates incompleteness of isothermal solidification and bonding process.

3.2 Effects of microstructure on mechanical properties

The microhardness analyses of the bonds made at 950, 1000, and 1050 °C are illustrated in Fig. 5. The main trend shows that the structure of profiles is split up into five distinguished regions. As predicted, the hardness of Ti-6Al-4 V is measured about 360 VHN. Adjacent to the Ti alloy, the hardness value markedly dropped to about 250–260 VHN which is alike for all specimens. It is considered that diffusion of Cu and Ni into the Ti alloy and stabilizing of β phase lead to a meaningful reduction in hardness value of this region. In the center of the joints, hardness value steeply increases; however, it is different for each sample. The value for the sample made at 950 °C stood at 340 VHN while with increase in bonding temperature to 1000 °C, microhardness value reached to 380 VHN. It is believed that formation of Ni-rich eutectic phases, including β_1 (NiTi), Δ (CuNiTi), and ι (Ni_3Ti), caused such rise in the center of joint zone. The measurements also indicate that the hardness value of joint center for the bonds made at 1050 is far lower than that of others so that it fluctuated at 300 VHN within the joint center. This can be due to the type of eutectic structure, containing γ (Ni, Cu) phase, and presence of microvoids and microcracks at the interface. Sticking to the stainless steel, a boom in hardness value is observed which may be attributed to the formation of various intermetallic compounds with Fe, Cu, Ti, Ni, and Cr elements. Finally, the hardness value of 160 VHN signifies presence of the Fe alloy at the end of joint. Considering the hardness test, formation of different eutectic structures in the center of joint is the main reason in different distribution of hardness values in the joint zone.

The stress-strain curves of bonded samples are given in Fig. 6. As clear in the diagram, the maximum value of shear strength is obtained for the bond made at 1000 °C (385 MPa) while with increase of bonding temperature, shear strength sharply declines so that a bond made at 1050 °C has the minimum value (257 MPa). Completion of TLP bonding process and formation of strengthening phases at the interface can be the key factors for increasing of shear strength value in lower bonding temperatures whereas samples bonded with higher temperatures are highly affected by incompleteness of isothermal solidification and existence of microcracks in the joint zone.

Fig. 5 Microhardness profiles of bonded samples at 950 °C (a), 1000 °C (b), 1050 °C (c)



3.3 Fractography

Identification of intermetallic compounds in the joint zone is not possible by EDS analysis and therefore, X-ray diffraction was employed for this purpose. X-ray diffraction patterns of fractured surfaces of bonded samples at 950, 1000, and 1050 °C are given in Fig. 7. The experiment approves presence of NiTi, CuTi, CuNiTi, and β -Ti on the Ti alloy side

while the fractured surface of stainless steel consists of FeTi and Fe_4Cu_3 for the bond made at 950 °C. The results also indicate formation of Ni_3Ti , CuNiTi, NiTi, β -Ti, and Cu_2Ti phases on the Ti side and Fe_2Ti , Cr_2Ti , and Fe_4Cu_3 on the SS side at 1000 °C. It is clear that intermetallic productions in the joint zone of this specimen are more than that of the sample bonded at 950 °C. Ni_3Ti , CuNiTi, β -Ti, and Ni are detected on the Ti alloy side for the bond made at 1050 °C and presence of

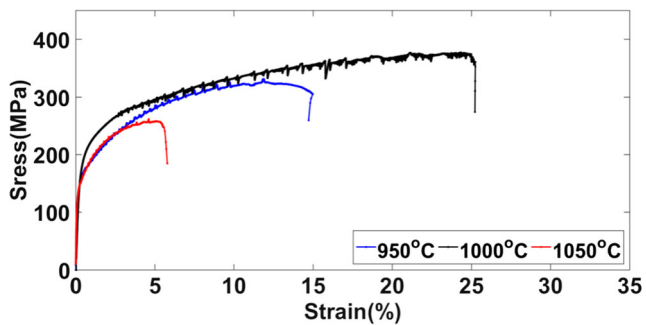


Fig. 6 Shear tensile stress-strain curves of bonded samples

Fe_2Ti , Fe_4Cu_3 , and Cu is proved on the SS side. As specified by XRD, presence of Cu and Ni at the interface can be attributed to incompleteness of bonding process for this sample. Another point should be noted is weak peak intensities of FeTi , Fe_2Ti , and Cr_2Ti in the XRD spectrum signifying low amount of these brittle intermetallics at the interface. As expected, presence of the interlayer in the joint area prevents from direct contact of Ti-6Al-4 V/stainless steel and impedes

formation of the brittle intermetallic compounds deteriorating mechanical properties of the bonds. It should be noted that the grain size and orientation significantly affect the peak intensity of the XRD plots. Hence, the XRD experiment was done for each sample three times in different locations of fracture surface to confirm the results. The experiment outcomes showed us that the general results are the same given in this paper.

Fracture morphologies of bonded joints are presented in Fig. 8. For the sample bonded at 950 °C, the fracture morphology shows a sign of combination of ductile and cleavage modes. Presence of river patterns on the surface would be a proof for participation of cleavage mode in the fracture mechanism. With increase of bonding temperature to 1000 °C, the appearance of fractured surface indicates a ductile failure mode. Ductile fracture in this sample can be due to formation of Ni-rich strengthening phases and absence of brittle intermetallics at the interface. As the bonding temperature increases to higher values, the fracture morphology completely changed. As observed in Fig. 8 d, the fractograph suggests a

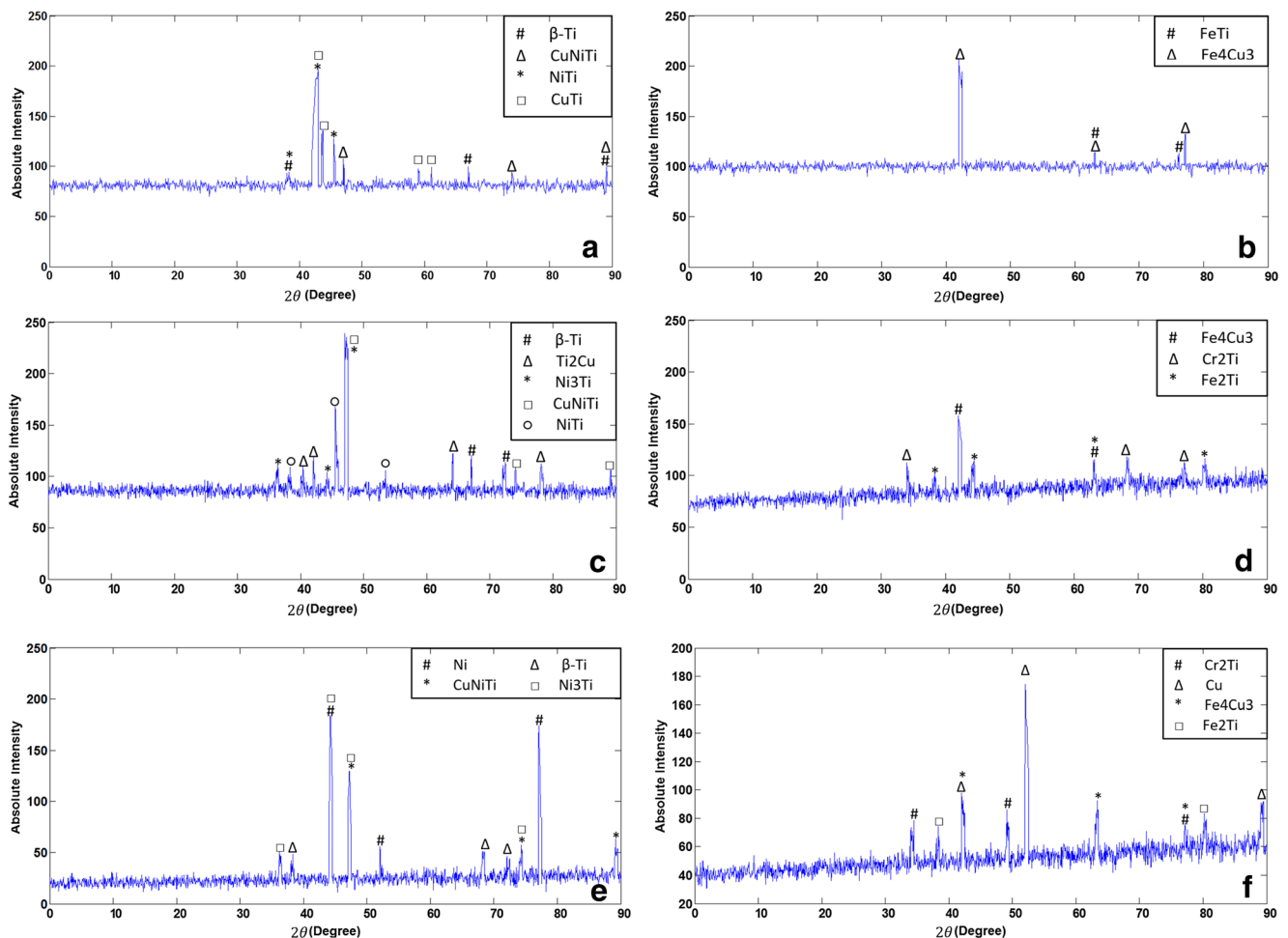


Fig. 7 XRD spectrums of fractured surfaces. **a** Ti side (950 °C). **b** Steel side (950 °C). **c** Ti side (1000 °C). **d** Steel side (1000 °C). **e** Ti side (1050 °C). **f** Steel side (1050 °C)

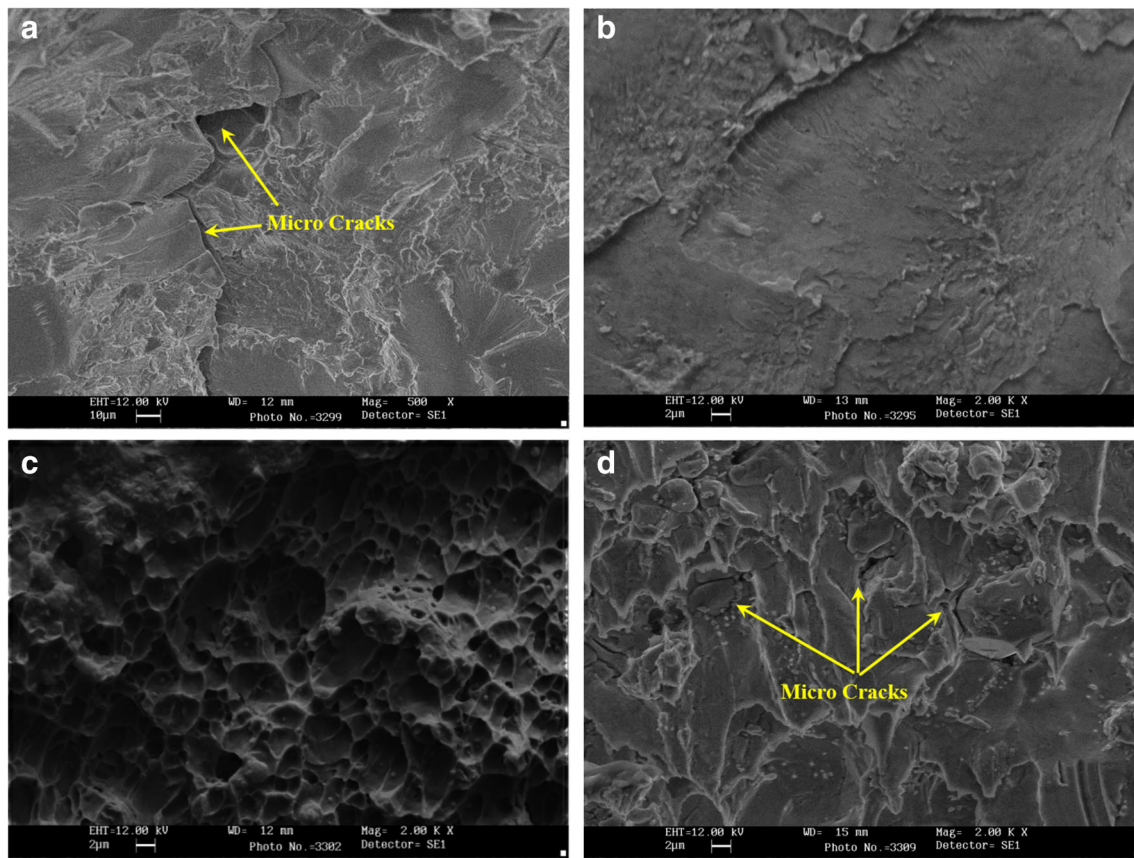


Fig. 8 a Fractured surface for the bonds made at 950 °C. b River-pattern shape at 950 °C. c Fractured surface for the bonds made at 1000 °C. d Fractured surface for the bonds made at 1050 °C

brittle fracture mode which can be due to presence of the voids and the microcracks in the joint zone. Two main factors are the reasons for microcrack and void formation at the interface. The incompleteness of bonding process and athermal solidification of remaining liquid leads to a shrinkage in the joint zone and as a result, the interface becomes susceptible to microcrack formation. On the other side, the excessive formation of brittle intermetallics at the interface facilitates the crack propagation. Hence, it is concluded that a suitable selection of bonding temperature (1000 °C) is needed to create a sound metallurgical joint with a complete bonding process and no inordinate intermetallic compounds.

4 Conclusion

In this work, TLP bonding of Ti-6Al-4 V to stainless steel 316 L using simultaneously both Cu and Ni interlayers with bonding temperatures of 950, 1000, and 1050 was carried out successfully. The following conclusions are drawn:

1. Interdiffusion of elements such as Cu, Ti, Ni, and Fe caused formation of eutectic phases at the interface.

2. An individual eutectic transformation at the interface was happened for each specimen in a specific bonding temperature
3. Increasing bonding temperature to 1050 °C led to formation of microvoids and microcracks in the joint zone.
4. Weak peak intensities of FeTi, Fe₂Ti, and Cr₂Ti in the XRD spectrum indicate low amount of these brittle intermetallic compounds in the joint zone. It is believed that presence of the interlayer in the joint area impedes formation of the brittle intermetallics deteriorating strength of the bonds.
5. With increase of bonding temperature, the shear strength was dramatically decreased which can be attributed to presence of microcracks and incompleteness of bonding process.

References

1. Lee JG, Lee M-K (2017) Microstructure and mechanical behavior of a titanium-to-stainless steel dissimilar joint brazed with Ag-Cu alloy filler and an Ag interlayer. *Mater Charact* 129:98–103
2. Guo S, Zhou Q, Xu P, Gao Q, Luo T, Peng Y, Kong J, Wang K, Zhu J (2017) Study on lightweight design and connection of dissimilar

- metals of titanium alloy TC4/T2 copper/304 stainless steel. International Conference on Intelligent Computing for Sustainable Energy and Environment pp 229–237
3. Sahasrabudhe H, Harrison R, Carpenter C, Bandyopadhyay A (2015) Stainless steel to titanium bimetallic structure using LENS™. *Addit Manuf* 5:1–8
 4. Pardal G, Ganguly S, Williams S, Vaja J (2016) Dissimilar metal joining of stainless steel and titanium using copper as transition metal. *Int J Adv Manuf Technol* 86(5):1139–1150
 5. Yang D, Luo Z, Xie G, Misra R (2018) Effect of interfacial compounds on mechanical properties of titanium–steel vacuum roll-cladding plates. *Mater Sci Technol* 34(14):1–10
 6. Tomashchuk I, Grevey D, Sallamand P (2015) Dissimilar laser welding of AISI 316L stainless steel to Ti6–Al4–6V alloy via pure vanadium interlayer. *Mater Sci Eng A* 622:37–45
 7. Muralimohan CH, Ashfaq M, Ashiri R, Muthupandi V, Sivaprasad K (2016) Analysis and characterization of the role of Ni interlayer in the friction welding of titanium and 304 austenitic stainless steel. *Metall Mater Trans A* 47(1):347–359
 8. Chen H-C, Bi G, Lee BY, Cheng CK (2016) Laser welding of CP Ti to stainless steel with different temporal pulse shapes. *J Mater Process Technol* 231:58–65
 9. Wang T, Zhang B, Feng J (2014) Influences of different filler metals on electron beam welding of titanium alloy to stainless steel. *Trans Nonferrous Met Soc China* 24(1):108–114
 10. Velmurugan C, Senthilkumar V, Sarala S, Arivarasan J (2016) Low temperature diffusion bonding of Ti-6Al-4V and duplex stainless steel. *J Mater Process Technol* 234:272–279
 11. Kaya M, Kılıç M, Kırık İ, Karakurt EM, Gülenç B (2017) Diffusion bonding between Ti-6Al-4V alloy and interstitial free steel. *Mater Werkst* 48(7):661–665
 12. Li P, Li J, Xiong J, Zhang F, Raza SH (2012) Diffusion bonding titanium to stainless steel using Nb/Cu/Ni multi-interlayer. *Mater Charact* 68:82–87
 13. Yıldız A, Kaya Y, Kahraman N (2016) Joint properties and micro-structure of diffusion-bonded grade 2 titanium to AISI 430 ferritic stainless steel using pure Ni interlayer. *Int J Adv Manuf Technol* 86(5):1287–1298
 14. Balasubramanian M (2016) Characterization of diffusion-bonded titanium alloy and 304 stainless steel with Ag as an interlayer. *Int J Adv Manuf Technol* 82(1):153–162
 15. Balasubramanian M (2015) Development of processing windows for diffusion bonding of Ti–6Al–4V titanium alloy and 304 stainless steel with silver as intermediate layer. *Trans Nonferrous Met Soc China* 25(9):2932–2938
 16. Balasubramanian M (2015) Application of Box–Behnken design for fabrication of titanium alloy and 304 stainless steel joints with silver interlayer by diffusion bonding. *Mater Des* 77:161–169
 17. Mukherjee AB, Laik A, Kain V, Chakravarty JK (2016) Shrinkage-stress assisted diffusion bonds between titanium and stainless steel: a novel technique. *J Mater Eng Perform* 25(10):4425–4436
 18. Wang F-L, Sheng G-M, Deng Y-Q (2016) Impulse pressuring diffusion bonding of titanium to 304 stainless steel using pure Ni interlayer. *Rare Metals* 35(4):331–336
 19. Jalali A, Atapour M, Shamanian M, Vahman M (2018) Transient liquid phase (TLP) bonding of Ti-6Al-4V/UNS 32750 super duplex stainless steel. *J Manuf Process* 33:194–202
 20. Norouzi E, Atapour M, Shamanian M (2017) Effect of bonding time on the joint properties of transient liquid phase bonding between Ti–6Al–4V and AISI 304. *J Alloys Compd* 701:335–341
 21. Kundu S, Thirunavukarasu G, Chatterjee S, Mishra B (2015) Effect of bonding temperature on phase transformation of diffusion-bonded joints of duplex stainless steel and Ti-6Al-4V using nickel and copper as composite intermediate metals. *Metall Mater Trans A* 46(12):5756–5771
 22. Kundu S, Chatterjee S (2008) Characterization of diffusion bonded joint between titanium and 304 stainless steel using a Ni interlayer. *Mater Charact* 59(5):631–637
 23. Gupta KP (2002) The Cu-Ni-Ti (copper-nickel-titanium) system. *J Phase Equilibria* 23(6):541–547

Publisher's note Springer Nature remains neutral with regard to jurisdictional claims in published maps and institutional affiliations.